

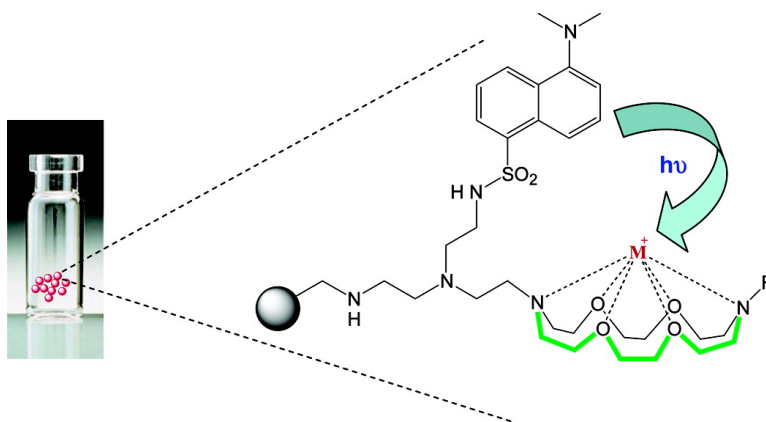
Article

Library Preparation of Derivatives of 1,4,10,13-Tetraoxa-7,16-diazacycloctadecane and Their Fluorescence Behavior for Signaling Purposes

I. A. Rivero, T. Gonzalez, G. Pina-Luis, and M. E. Diaz-Garcia

J. Comb. Chem., **2005**, 7 (1), 46-53 • DOI: 10.1021/cc049897c • Publication Date (Web): 06 November 2004

Downloaded from <http://pubs.acs.org> on March 22, 2009



More About This Article

Additional resources and features associated with this article are available within the HTML version:

- Supporting Information
- Links to the 2 articles that cite this article, as of the time of this article download
- Access to high resolution figures
- Links to articles and content related to this article
- Copyright permission to reproduce figures and/or text from this article

[View the Full Text HTML](#)



ACS Publications
 High quality. High impact.

Library Preparation of Derivatives of 1,4,10,13-Tetraoxa-7,16-diaza-cyclooctadecane and Their Fluorescence Behavior for Signaling Purposes

I. A. Rivero,^{*,†} T. Gonzalez,[†] G. Pina-Luis,[†] and M. E. Diaz-Garcia[‡]

Graduate Center & Research, Technological Institute of Tijuana, P.O. 1166,
Tijuana, 22000 B.C. México, and Department of Physical and Analytical Chemistry,
Faculty of Chemistry, University of Oviedo, Av. Julián Clavería 8, 33006 Spain

Received June 16, 2004

In the present work, we report the library preparation on solid supports of 20 derivatives of 1,4,10,13-tetraoxa-7,15-diaza-cyclooctadecane **1(a–e)(w,x,y,z)** carrying a fluorescent dansyl group. The sensing fluorescence behavior of these materials toward alkali and alkali earth metal ions was studied by packing the beads into a conventional flow-through cell in a FIA (flow injection analysis) approach. The fluorescence emission of these materials' responses shows a fluorescence increase to Li⁺, Na⁺, K⁺, NH₄⁺, Ca²⁺, and Mg²⁺ with maximum sensitivity for Mg²⁺ over the rest of the ions. The analytical potential of these materials is outlined, and the sensing response mechanism, based on a photoinduced electron-transfer process, is proposed.

Introduction

The development of supramolecular systems able to bind selectively and reversibly an ion or a molecule with a concomitant change in their spectral properties is an important area of current sensing research.^{1–5} The design of the multicomponent or modular approach represents a straight and rational way to the design of a molecular sensor for any kind of analyte. According to this approach, a three-module format, “lumophore–spacer–receptor”, results in an inter-component process which may be established or interrupted between the receptor subunit and the luminescent moiety in such a way that the light emission is quenched or revived upon the recognition event. The luminescent mechanism that has yielded the greatest harvest so far for sensing applications is photoinduced electron transfer (PET). The principle of luminescent PET sensing is illustrated in Figure 1. In this context, the use of supramolecular host–guest interactions may provide the basic recognition function (e.g., the well-known affinity between a crown ether and alkali/alkaline earth cations) acting as electron donor and the fluorophore playing the role of an acceptor.⁶ The design and synthesis of a wide variety of PET chemosensors based on macrocyclic ethers as receptors for ionic and nonionic species carrying different fluorophores is an area of intense activity and of tremendous potential significance.^{7–12} Immobilization of fluorescent chemosensors on solid supports would result in improved analytical properties, such as continuous readout, increased sensitivity, lower reagent consumption, and the possibility of using the sensor in solvents in which the free molecule may display low solubility. This concept, despite

its great scope for the development of luminescent chemosensors, has been scarcely exploited, and only few examples of sensor applications of immobilized PET chemosensors have been reported so far.^{13–16} We describe here our recent work on the synthesis of fluorescent chemosensors for alkali/alkaline earth cations in water. Our design was based on 1,4,10,13-tetraoxa-7,16-diaza-cyclooctadecane derivative receptors to which a dansyl fluorophore was covalently linked and generated via solid-phase library synthesis.¹⁷ The structural, fluorescence, and metal ion binding properties of these chemosensors are described.

Results and Discussion

Lariat Ether Dansyl Immobilization. Three representative resins, Wang, Argopore, and Argogel were chlorinated with BTC/PPh₃P¹⁸ to obtain the respective chlorinated resins¹⁹ **3(x,y,z)**, which were converted to the trisamine-based derivatives **4(x,y,z)** (Scheme 1). Different protocols (A, B, C, D, vide infra) were assayed to introduce the trisamine group, and results demonstrated that the conversion yield was optimal using K₂CO₃/KI, the reaction conditions of the B procedure. The commercial resin PS-trisamine, **4w**, was used throughout this investigation for comparative purposes.

The **4(w,x,y,z)** resins were then coupled to the high quantum yield fluorescent molecule dansyl chloride **5** according to the route outlined in Scheme 2. The resins were suspended in CH₂Cl₂ with dansyl chloride to form dansylated resins **6(w,x,y,z)**. Upon reaction, **6(w,x,y,z)** were swelled in dry CH₃CN and reacted with 1,2-bis(2-iodoethoxy)ethane in CH₃CN solution containing anhydrous Na₂CO₃ to build up the arms of the crown ether structure on the primary amine group available. The resulting resins **7(w,x,y,z)** were finally treated with the corresponding alkyl- or arylamine (aniline,

* To whom correspondence should be addressed. E-mail: irivero@tectijuana.mx.

† Technological Institute of Tijuana.

‡ University of Oviedo.

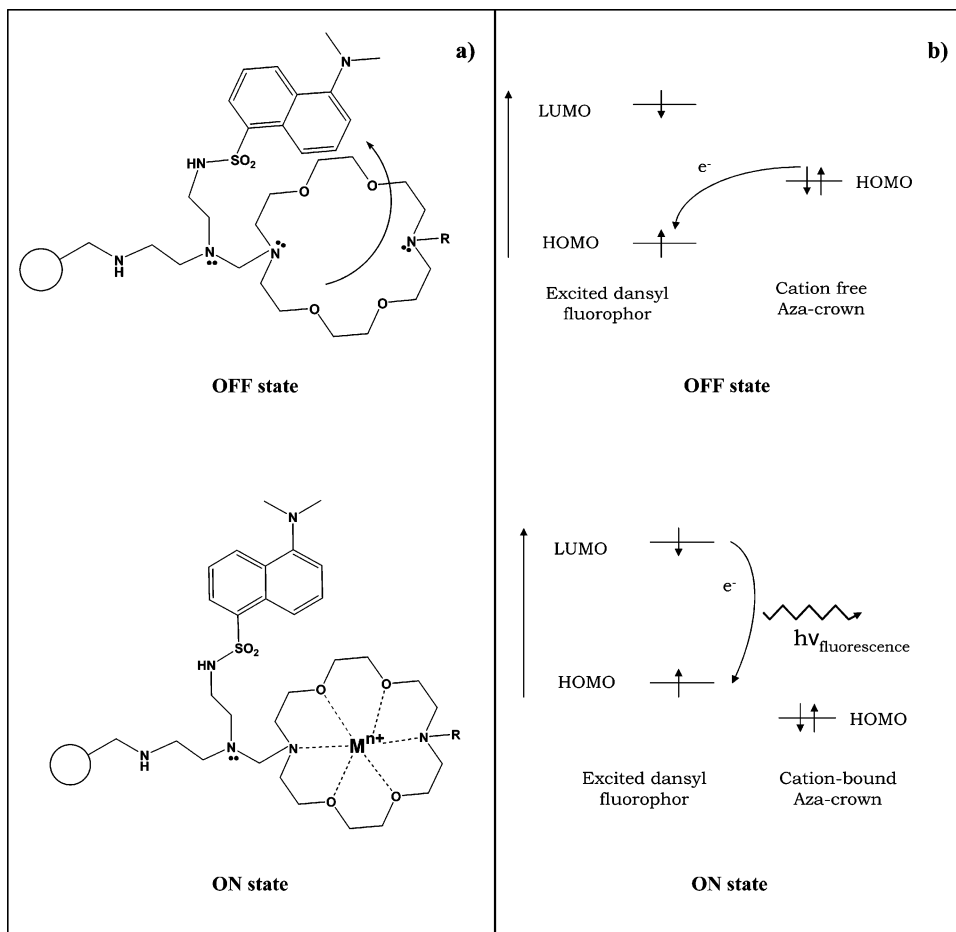
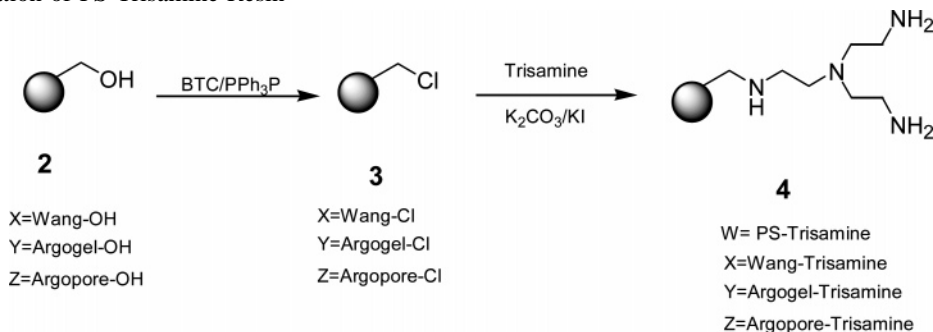


Figure 1. (a) Schematic representation of the thermodynamic conditions for PET sensing; (b) orbital diagram illustrating the occurrence of the PET process.

Scheme 1. Preparation of PS-Trisamine Resin



benzylamine, 4-phenylbutylamine, butylamine, and pentylamine) to obtain the resins **1**.

The different reaction steps were monitored by IR and fluorescence spectroscopy. In addition, a simple method based on direct-insertion mass spectrometry with electronic impact, developed in our group,²⁰ was also used for the analysis of polymer-supported species. The instrument was operated at high temperature and high vacuum, which resulted in the thermal cleavage of the benzylic position in the resins, thus liberating the substrate attached to the resin. The mass spectra gave information about the products without degradation, which was very useful for characterizing intermediates in the overall synthetic process.²⁰ The library design shown in Table 1 represents a 4×5 array of Lariat ether beads with diversity achieved by variations in the solid support and the amine substituents.

Fluorimetric Characterization. Constant monitoring of the different synthesis steps was carried out by on-bead fluorescence. Resins were transferred to a conventional flow-through fluorescence cell, and spectra were obtained directly from the dry resin beads. In Figure 2, the fluorescence emission spectra of the intermediates **4w** (PS-trisamine resin), **6w** (PS trisamine dansyl resin), and the final product **1bw** (PS-trisamine dansyl crown ether resin) are shown. The remaining library PS intermediates and final products for the above synthesis steps showed a similar spectral luminescence pattern.

As can be seen, incorporation of the dansyl probe onto the resin **4w** is evidenced by a drastic red shift in the spectral characteristics of **6w**, indicating the presence of the dansyl sulfonamide on the solid support. In fact, the excitation and fluorescence emission bands of **6w** are consistent with those

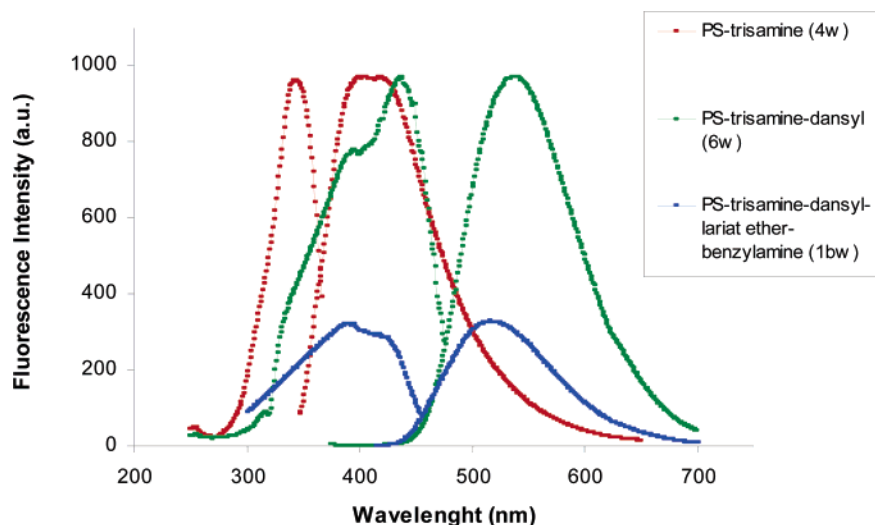


Figure 2. Excitation and emission spectra of dry resin beads of the intermediates **4w**, **6w**, and the final product, **1bw**.

Scheme 2. Reaction Sequence for the Synthesis of PS-Trisamine Dansyl Lariat Ether-(Alkyl/arylamine) Resins **1**

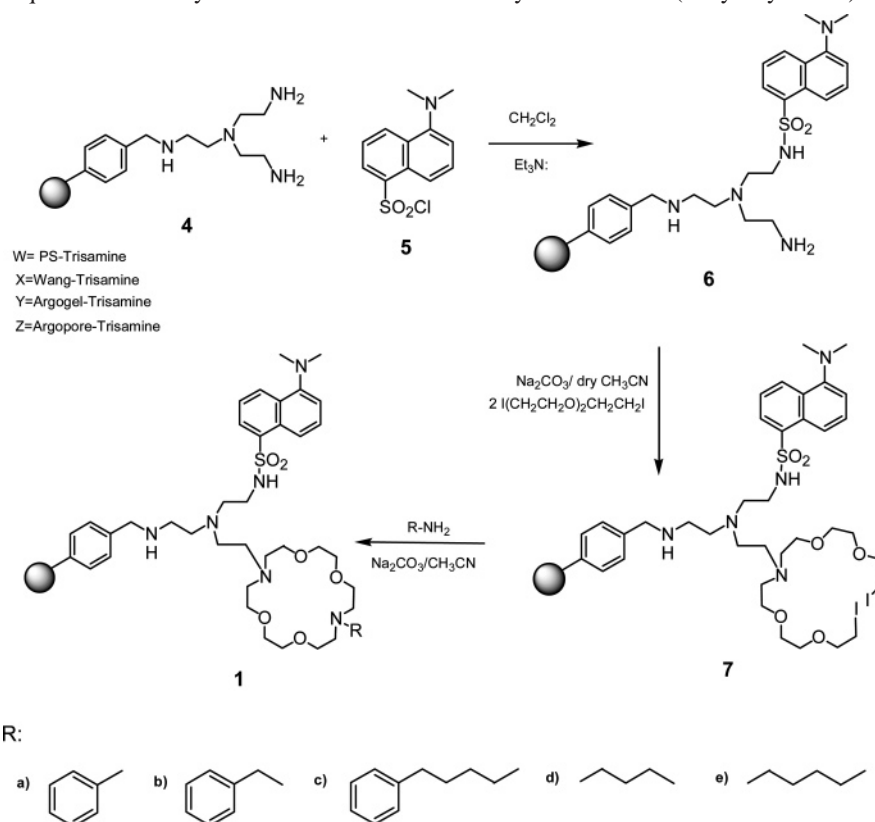


Table 1. Library Design

R-group/resin	PS-trisamine	Wang resin	ArgoGel	ArgoPore
phenyl	1aw	1ax	1ay	1az
benzyl	1bw	1bx	1by	1bz
4-phenylbutyl	1cw	1cx	1cy	1cz
butyl	1dw	1dx	1dy	1dz
amyl	1ew	1ex	1ey	1ez

of 1-(dimethylamino)-5-naphthalenesulfonamide in organic solvents, such as DMF, DMSO, CH₃CN, or 2-propanol, with a maximum emission at ~530 nm.^{21,22}

Similar results were observed for those materials prepared from Argogel, Argopore, and Merrifield resins. With the starting (**4x,y,z**) resins, excitation and emission bands were

obtained in the range 342–363 and 403–423 nm, respectively, while for dansylated resins (**6x,y,z**) fluorescence maximums were observed at 436–502 and 538–596 nm, respectively. Fluorescence spectral data for all products **1(a–e)(w,x,y,z)** are summarized in Table 2.

It was noteworthy that several interactions, working in cooperation, resulted in a low fluorescence intensity of all derivatives **1(a–e)(w,x,y,z)**, as compared to that of dansylated resins **6(w,x,y,z)**, with a remarkable lower intensity for resins **1(a,b,c)** (R = arylamine). The dansyl group and the substituted crown ether are appended to the resin through ethylene–amine linkages which bring them into proximity; thus, fluorescence from the dansyl fluorochrome is quenched

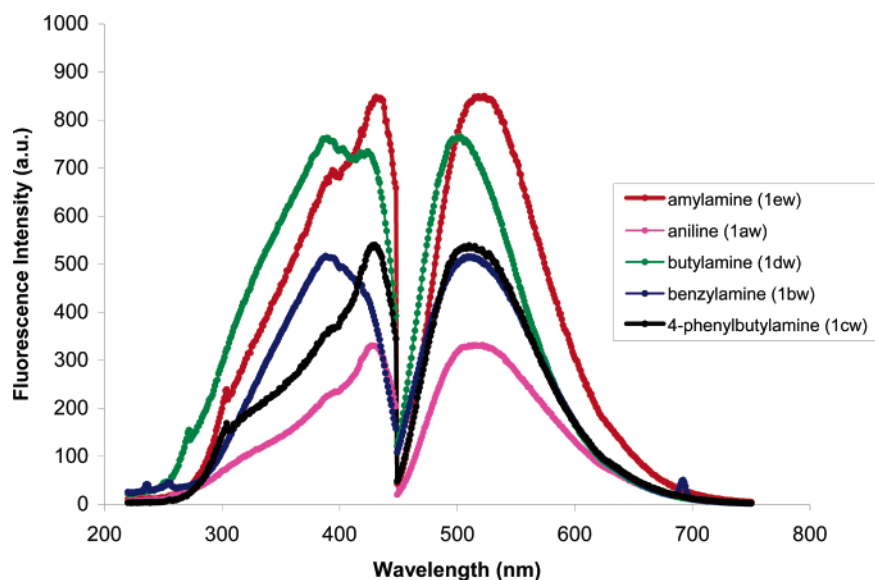
Table 2. Spectral Data of Library Materials **1(a–e)(x–w)**

item (1 $\alpha\omega$)	IF, au	exc max	em max	Stokes' shift
1aw	332	427	516	89
1ax	254	409	511	102
1ay	301	413	528	115
1az	377	435	530	95
1bw	518	388	510	122
1bx	437	396	547	151
1by	506	394	538	144
1bz	624	397	539	142
1cw	542	428	508	80
1cx	417	433	545	112
1cy	453	414	552	138
1cz	598	421	556	135
1dw	767	389	500	111
1dx	701	396	519	123
1dy	623	403	521	118
1dz	797	392	535	143
1ew	852	431	522	91
1ex	761	427	539	112
1ey	834	446	553	107
1ez	916	440	548	108

by photoelectron transfer (PET) from its crown ether counterpart (see Figure 1). The nature of the substituent R group on the crown ether proved to be important in the ability to quench dansyl fluorescence. The quenching efficiency of the alkyl substituents was of similar magnitude for both **d** and **e** substituents, while a higher quenching efficiency was observed for the aryl substituents, **a**, **b**, and **c**. Furthermore, upon increasing the distance between the aryl group and the crown ether, quenching by photoelectron transfer became less efficient, and a concomitant increase in the overall fluorescence emission was observed. This behavior can be attributed to the flexible nature of the functionalized tetramine, which may result in the formation of a coplanar structure that promotes π -stacking interactions between the aryl substituent (R) and the fluorophore (dansyl), and thus, the probability of the PET process is enhanced.²³ Figure 3 illustrates the influence of R groups on the fluorescence intensity of **1(a–e)(w)** final products, and similar results were also observed in the case of Wang-, Argogel-, and Argopore-based products.

Metal Ion Recognition Properties of Crown Ether Dansyl Resins. Evaluation of the final materials **1(a–e)(w,x,y,z)** as fluorescent signaling receptors for alkali/alkaline earth cations Li^+ , Na^+ , K^+ , Ca^{2+} , Mg^{2+} , and NH_4^+ was achieved by packing the corresponding beads into a conventional flow-through fluorescence cell and using a continuous flow injection setup (Figure 4).

In the absence of cationic metal guests, luminescence from the **1bw** derivative was low due to the PET process (Figure 5A), as described above. Cation complexation resulted in large increases in luminescence intensity. These results seemed to indicate that the sensing materials worked as a result of conformational changes upon metal complexation.²⁴ In the absence of a metal ion, the dansyl and the crown ether units can adopt a more or less cofacial orientation, which is favorable for electron transfer to the HOMO orbital of the dansyl. Complexation of cations forced the crown ether unit away from the dansyl lumophore, thereby destabilizing putative cofacial configurations of the components.²⁴ The change in conformation prevented intramolecular electron transfer from the crown ether to the dansyl fragment and restored the luminescence of the latter (Figure 1). The photophysical changes upon cation binding can also be described in terms of orbital energies (see right side Figure 1). Upon excitation of the dansyl fluorophore, an electron of the highest occupied molecular orbital (HOMO) is promoted to the lowest unoccupied molecular orbital (LUMO), which allows PET from the HOMO of the donor (free cation receptor) to that of the fluorophore, thus quenching the fluorescence of the latter. Upon cation binding, the redox potential of the donor is raised so that the HOMO becomes lower in energy than that of the fluorophore. As result, PET is no longer possible, and fluorescence quenching is suppressed. This mechanism is illustrated in the molecular orbital scheme in Figure 1. The increase in luminescence intensity was observed to scale with the nature of the metal ion: Ca^{2+} , Li^+ , Na^+ , K^+ , and NH_4^+ gave ~36% increase in fluorescence intensity, while exposure to Mg^{2+} yielded 200% fluorescence increase, calculated according to the expression $\Delta I\% = I_b$

**Figure 3.** Fluorescence spectra of dry resin beads of final products with different amine substituents, **1(a–e)(w)**.

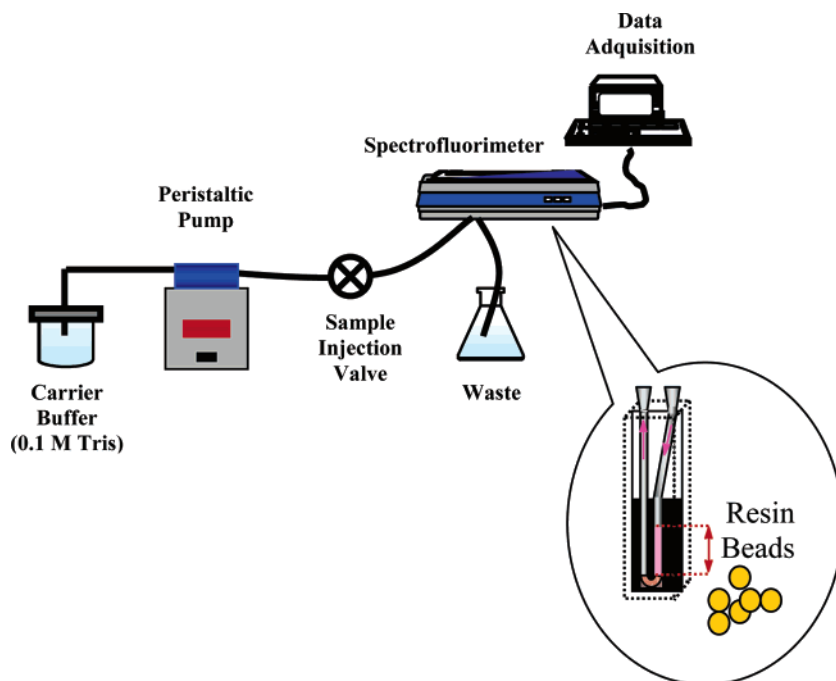


Figure 4. Flow injection setup for screening the sensing beads.

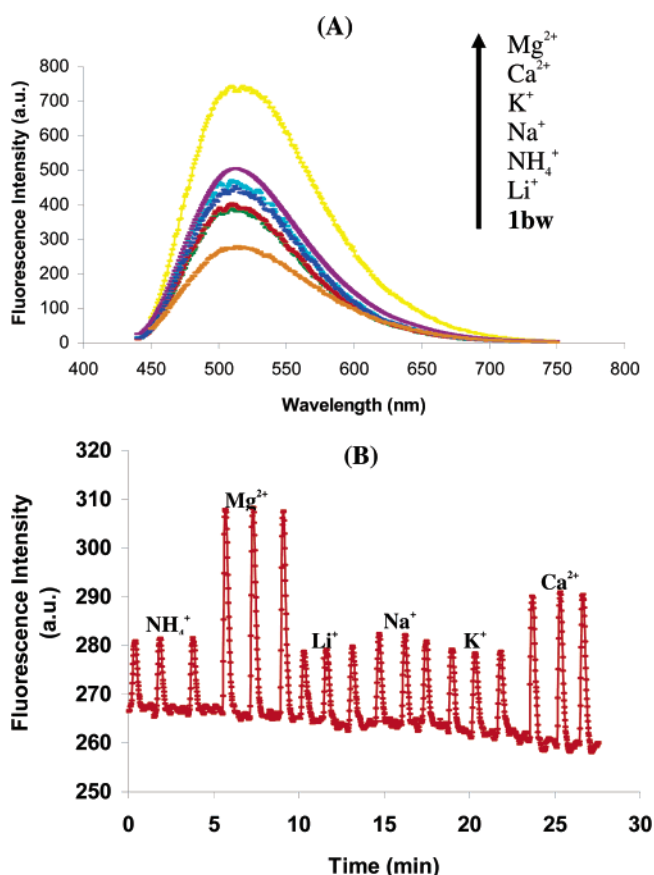


Figure 5. (A) Fluorescence emission spectral changes of PS-trisamine dansyl crown ether **1bw** with (0.1 M) and without metal cations and (B) successive response and recovery cycles of the **1bw** derivative sensing material exposed to alkali metals (2.5 μmol) in a flow injection approach (Tris 1 M buffer pH 8, $\lambda_{\text{exc}} = 390 \text{ nm}$, $\lambda_{\text{em}} = 511 \text{ nm}$).

– $I_f/I_b \times 100$, in which I_f and I_b corresponded to the fluorescence intensity of the free and to the metal-bound receptor, respectively. Qualitatively, this behavior could be

Table 3. Ionic Radii, Softness Parameters σ , Surface Charge Densities, and Entropies $-\Delta S^\circ$ of Hydration of Some Alkali and Alkali-Earth Metal Cations²⁵

cation	ionic radius (\AA)	softness (σ)	surface charge density ($Z \text{\AA}^{-2}$) ($Z = 1$ or 2)	$-\Delta S^\circ$ (e.u.)
Li^+	0.78	0.247	0.13	25.5
Na^+	0.98	0.211	0.085	17.5
K^+	1.33	0.232	0.045	9.5
NH_4^+	1.48	0.229		
Ca^{2+}	1.06	0.180	0.14	50
Mg^{2+}	0.78	0.167	0.26	64

attributed to the separation distance between the lumophore and the crown ether being varied due to Coulombic effects, which are stronger for the small, high-charge density metal ion Mg^{2+} , and from the larger gain in entropy on removal of the solvation shell for Mg^{2+} , as compared to the other metal ions (see Table 3).

In Figure 5B, the flow response–time profile of the **1bw** material as signaling phase of metal ion standards, each injected in triplicate, is shown. Reaction of the different **1(a–e)(w)** materials with the selected metal ions demonstrated that the restoration of fluorescence was not dependent on the nature of the crown ether substituent, and the fluorescence enhancement followed a similar trend with all the metal ions assayed. See Figure 6, in which the fluorescence intensity of the **1(a–e)(w)** materials was normalized with respect to that of the magnesium-bound material.

The reversibility and reproducibility of the response are adequate enough to consider these simple systems as efficient fluorosensors for alkali and alkaline-earth cations. It is gratifying to note that metal–fluorophore communication through a PET process can be directly developed on solid phase, which could lead to a practically useful sensing device. Having established the basic requisite of building blocks needed for the potential sensing of magnesium, work is currently underway in our laboratory, and results will be reported in due course.

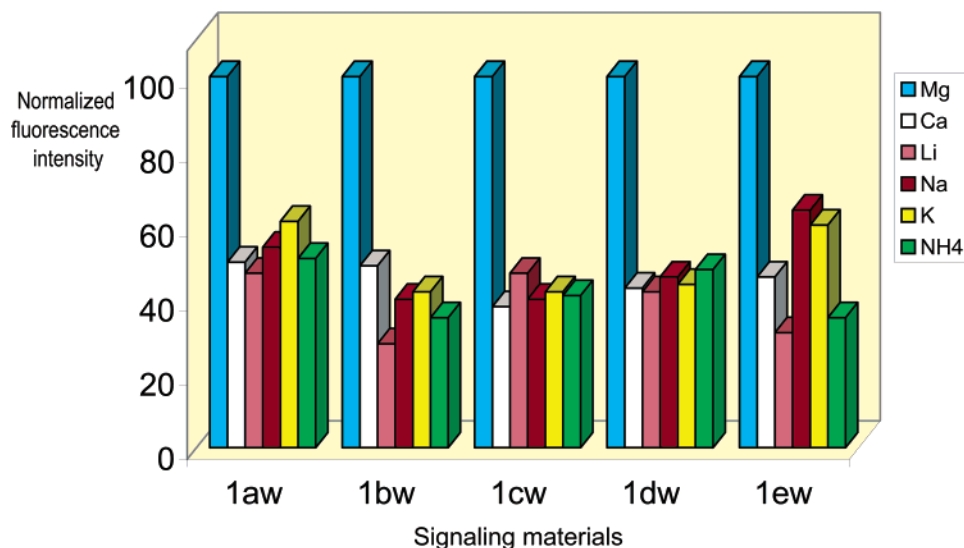


Figure 6. Normalized fluorescence response of the 1(a–e)(w) library toward alkali- and alkali-earth metal ions.

In conclusion, Lariat ether dansyl resins were synthesized, and their sensing properties for alkali and alkaline-earth cations were evaluated. The results demonstrate our main design principle that chemosensors based on the PET process can be developed on solid supports and that recognition can be fine-tuned by screening libraries that contain a variable recognition domain. The development of these types of sensing systems on solid supports will no doubt produce novel prototype fluorescent chemosensor devices of the future.

Experimental Section

Materials. Wang-OH (**2x**), ArgoGel-OH (**2y**), ArgoPore-OH (**2z**), and PS-trisamine (**4w**) resins used in this work were purchased from Argonaut Technologies Inc. and have loadings of 1.06, 0.47, 0.96, and 1.4 mmol/g. All other reagents, unless specified otherwise, were purchased from Aldrich. All other chemicals, buffers, and solvents were of analytical reagent grade and were used without further purification. All aqueous solutions were prepared using deionized water. Standards working solutions of Na^+ , Li^+ , K^+ , Mg^{2+} , and NH_4^+ (as chloride salts) at different concentrations were prepared in the buffer solution.

Instrumentation. Melting points were obtained on an Electrothermal 88629 apparatus and are uncorrected. Infrared (IR) spectra were recorded on a Perkin-Elmer FT-IR 1600 spectrometer. ^1H and ^{13}C nuclear magnetic resonance spectra were recorded on a Varian Mercury 200 spectrometer in CDCl_3 with TMS as internal standard, at 200 and 50.289 MHz, respectively. Mass spectra were obtained on a Hewlett-Packard 5989 MS spectrometer at 70 eV by direct insertion. All fluorescence intensity measurements were made with a Shimadzu RF-5301 PC spectrometer. A single flow injection system equipped with a Hellma model 176.52 flow cell (25 μL) was used for assays. Beads were washed free of any starting materials and solvent and were placed into the flow-through cell. Measures of fluorescence intensity were obtained directly from the resin beads. All experiments were carried out at $20 \pm 2^\circ$.

Chlorination Method. Conversion of hydroxyl resins into chlorinated ones was carried out according to the chlorination

method described elsewhere.¹⁸ We applied some modification to the original procedure as follows: triphosgene (1.46 g) was added with constant stirring to a solution of triphenylphosphine (3.472 g) dissolved in CH_2Cl_2 at 0°C (1:2.7 stoichiometric molar ratio). Then the mixture was stirred for 20 min at 20°C , after which the solvent was removed in a vacuum. The crude white solid obtained was dissolved in 20 mL of CH_2Cl_2 to obtain the chlorination reagent solution. PS Wang, Argopore Wang, and Argogel Wang resins (150 mg), placed in parallel reactors, were swollen in CH_2Cl_2 (5 mL) and agitated for at least 30 min, then the vessels were drained, and the chlorination reagent solution (1 mL = 1 equiv chlorination solution) was added to the resins. Parallel Chemistry was carried out in a reactor, Quest Argonaut model SLN-210. Operation parameters in the equipment were as follows. Agitation parameters: mix event, 4.0 s; up stroke, 3.0 s; % upward, 80%. Temperature, 20°C . Volume, 5 mL. Automated solvent wash, CH_2Cl_2 (3×5 mL), methanol (3×5 mL), and finally CH_2Cl_2 (3×5 mL). Agitation, 5 min; and drain time, 25 s. The resins were removed from the corresponding vessels and were dried off under high vacuum for 18 h. Quantitative recoveries of the resins were obtained as white solids, and the conversion (%) was evaluated by the Volhard method.²⁶

Chlorinated Products. Wang-Cl (2x**).** 1.38 g (recovery 92%), conversion 95%. IR (KBr): 3025, 2923, 1602, 1509, 1491, 1446, 1238, 1024 cm^{-1} .

Argogel-Cl (2y**).** 1.42 g (recovery 95%), conversion 91%. IR (KBr): 3024, 2870, 1458, 1351, 1292, 1247, 1107 cm^{-1} .

Argopore-Cl (2z**).** 1.35 g (recovery 90%), conversion 93%. IR (KBr): 3018, 2929, 1605, 1494, 1454, 1266, 1181, 1100 cm^{-1} .

General Methods for the Synthesis of PS-Trisamine Based on Merrifield, Argopore, Argogel, and Wang Resins. Argopore-Cl, Argogel-Cl, and Wang-Cl resins were used under different reaction conditions to support trisamine.

Method A. Portions (350 mg) of the resins Argogel-Cl (0.165 mmol), Argopore-Cl (0.336 mmol), and Wang-Cl (0.352 mmol) were placed in the reaction tubes of the equipment and suspended in DMF (10 mL). Then K_2CO_3 (5 equiv) and trisamine (1.1 equiv) were added, and the mixture

was left to react at room temperature for 3 h, after which the resin was filtered and washed with H₂O (3 × 5 mL), DMF (3 × 5 mL), CH₃OH (3 × 5 mL), and CH₂Cl₂ (3 × 5 mL). Finally, the resin was dried under reduced pressure.

Method B. Portions (350 mg) of the resins ArgoGel-Cl (0.165 mmol), ArgoPore-Cl (0.336 mmol), and Wang-Cl (0.352 mmol) were placed in the reaction tubes of the equipment and suspended in DMF (10 mL). Then K₂CO₃ (2.5 equiv), KI (2.5 equiv), and trisamine were added (1.1 equiv), and the mixture was left to react at room temperature for 3 h, after which the resin was filtered and washed with H₂O (3 × 5 mL), DMF (3 × 5 mL), CH₃OH (3 × 5 mL), and CH₂Cl₂ (3 × 5 mL). Finally, the resin was dried under reduced pressure.

Method C. Portions (350 mg) of the resins ArgoGel-Cl (0.165 mmol), ArgoPore-Cl (0.336 mmol), and Wang-Cl (0.352 mmol) were placed in the reaction tubes of the equipment and suspended in NMP (10 mL). Then TMG (1 equiv) and trisamine were added (1.1 equiv), and the mixture was left to react at room temperature for 3 h, after which the resin was filtered and washed with H₂O (3 × 5 mL), NMP (3 × 5 mL), DMF (3 × 5 mL), CH₃OH (3 × 5 mL), and CH₂Cl₂ (3 × 5 mL). Finally, the resin was dried under reduced pressure.

Method D. In the reaction tubes of the equipment were placed 350 mg of the resin ArgoGel-Cl (0.165 mmol), ArgoPore-Cl (0.336 mmol), and Wang-Cl (0.352 mmol), and they were suspended in NMP (10 mL). Later, TMG (2 equiv) and trisamine were added (1.1 equiv), and the mixture was left to react at room temperature for 3 h, after which the resin was filtered and washed with H₂O (3 × 5 mL), NMP (3 × 5 mL), DMF (3 × 5 mL), CH₃OH (3 × 5 mL), and CH₂Cl₂ (3 × 5 mL). Finally, the resin was dried under vacuum. The percentage of conversion was determined by the Volhard method.¹⁹ To get the mass spectral data, the resins were treated with TFA/CH₂Cl₂ (1:1) for 30 min.

Wang-Trisamine (4x). 0.36 g (92%), conversion 95%. IR (KBr): 3424, 3025, 2915, 1601, 1222, 1447, 1107, cm⁻¹. ESI-MS (*m/z*): 147 [M + H]⁺, 130 [M - NH₂]⁺, 113 [M - 2NH₂]⁺.

ArgoGel-Trisamine (4y). 0.34 g (92%), conversion 93%. IR (KBr): 3446, 3011, 2922, 2870, 1598, 1450, 1255, 1104 cm⁻¹. ESI-MS (*m/z*): 147 [M + H]⁺, 130 [M - NH₂]⁺, 113 [M - 2NH₂]⁺.

ArgoPore-Trisamine (4z). 0.37 g (96%), conversion 97%. IR (KBr): 3439, 3025, 2922, 1601, 1454, 1250, 1104 cm⁻¹. ESI-MS (*m/z*): 147 [M + H]⁺, 130 [M - NH₂]⁺, 113 [M - 2NH₂]⁺.

General Method for the Synthesis of Trisamine-Dansyl-Supported Materials Based on Merrifield, Wang, Argopore, and Argogel Resins. PS-Trisamine-Dansyl (6w,x,y,z). In separate reaction vessels, PS-trisamine (250 mg, 1.15 mmol, 1 NH₂), ArgoGel-trisamine (250 mg, 0.11 mmol, 1 NH₂), ArgoPore-trisamine (250 mg, 0.22 mmol, 1 NH₂), and Wang-trisamine (250 mg, 0.22 mmol, 1NH₂) were suspended in dichloromethane (10 mL) under constant stirring for 30 min. TEA (1 equiv) was then added the mixture. A solution of dansyl chloride (1.1 equiv) in CH₂-Cl₂ (10 mL) was slowly added, and the mixture was refluxed

for 1 h. The mixture was filtered, and the residue was washed with MeOH/water (1:1) (3 × 10 mL), MeOH (3 × 10 mL), and CH₂Cl₂ (3 × 10 mL). The resins were dried under high vacuum. Polymer-supporting yields were calculated by the consumption of dansyl chloride.²⁶ The mass spectral data were obtained using a direct method.²⁰ Results demonstrated an overall yield of 92% for the conversion of **4** into **6**, which corresponds to a yield lower than 10% for byproducts (e.g., bis-dansylated resins) or unreacted **4**.

PS-Trisamine Dansyl (6w). 456 mg (88%), conversion 96%. IR (KBr): 3416, 2918, 1652, 1400, 1309 (Naph-SO₂), 1133 cm⁻¹. FI = 972 au, *E*_{em} = 538 nm, (*E*_{ex} = 436 nm). EI-MS (*m/z*): M⁺ 362 (5%), 250 (25%), 235 (21%).

Wang-Trisamine Dansyl (6x). 270 mg (93%), conversion 98%. IR (KBr): 3420, 2920, 1653, 1383, 1313 (Naph-SO₂), 1140 cm⁻¹. FI = 436 au, *E*_{em} = 577 nm, (*E*_{ex} = 486 nm). EI-MS (*m/z*): M⁺ 362 (7%), 250 (29%), 235 (35%).

Argogel-Trisamine Dansyl (6y). 263 mg (96%), conversion 93%. IR (KBr): 3440, 2920, 1653, 1383, 1300 (Naph-SO₂), 1106 cm⁻¹. FI = 495 au, *E*_{em} = 583 nm, (*E*_{ex} = 494 nm). EI-MS (*m/z*): M⁺ 362 (10%), 250 (32%), 235 (24%).

ArgoPore-Trisamine Dansyl (6z). 274 g (91%), conversion 95%. IR (KBr): 3440, 2926, 1656, 1383, 1323 (Naph-SO₂), 1146 cm⁻¹. FI = 217 au, *E*_{em} = 596 nm, (*E*_{ex} = 502 nm). EI-MS (*m/z*): M⁺ 362 (4%), 250 (21%), 235 (19%).

General Method for the Synthesis of Library of Trisamine Dansyl-Lariat Ether Supported Materials Based on Merrifield, Wang, Argogel, and Argopore Resins. PS-Trisamine Dansyl-Lariat Ether (1). The resin **6w** (250 mg, 0.5 mmol, 1 NH₂), **6x** (250 mg, 0.18 mmol, 1 NH₂), **6y** (250 mg, 0.1 mmol, NH₂), and **6z** (250 mg, 0.18 mmol, 1 NH₂) were allowed to swell in dry CH₃CN (10 mL) for 15 min under constant stirring in an argon atmosphere. A solution of 1,2-bis(2-iodoethoxy)ethane (2.2 equiv) in dry CH₃CN (10 mL) and Na₂CO₃ (5 equiv) was added to the mixture. The reaction was heated at 83 °C at constant stirring and continued to reflux for 24 h to give rise to the bis(iodo) derivative **7**. Compound **7** was cyclized with various primary amines using Na⁺ as the template to keep the chains together during the reaction. Using dry sodium carbonate in acetonitrile (2–3% solution), aniline, benzylamine, 4-phenylbutylamine, amylamine, or butylamine (1.1 equiv) were added, and the mixture was heated to reflux for 24 h. The suspension was filtered and washed with CH₃CN (1 × 10 mL), MeOH (1 × 10 mL), CH₂Cl₂ (1 × 10 mL), water (3 × 10 mL), MeOH (3 × 10 mL), and CH₂Cl₂ (3 × 10 mL). The solids **1(a–e)(w,x,y,z)** were recovered after drying under high vacuum. To get the mass spectra data, the resins were treated with TFA/CH₂Cl₂ (1:1) for 30 min. Results demonstrated an overall yield of 93% for the conversion of **7** into **1**, which corresponded to a yield lower than 8% for **7** byproducts.

PS-Trisamine Dansyl-Lariat Ether Aniline (1aw). (recovery 90%, conversion 97%). IR (KBr): 3422, 2929, 1654, 1579, 1458, 1321, 1133 cm⁻¹. FI = 332 au, *E*_{em} = 516 nm, (*E*_{ex} = 427 nm). ESI-MS (*m/z*): 657 [M - C₂H₄-NH₂ + H]⁺.

PS-Trisamine Dansyl-Lariat Ether Benzylamine (1bw). (recovery 90%, conversion 98%). IR (KBr): 3022, 2918, 1599, 1451, 1104 cm⁻¹. FI = 518 au, *E*_{em} = 510 nm, (*E*_{ex} =

388 nm). EI-MS (m/z): M^+ 424 (1%), 91 ($C_7H_7^+$) (100%). ESI-MS (m/z): 685 [$M - CH_2NH_2 + H$] $^+$.

PS-Trisamine Dansyl-Lariat Ether 4-Phenylbutylamine (1cw). (recovery 94%, conversion 96%). IR (KBr): 3018, 2923, 1576, 1458, 1137 cm^{-1} . FI = 542 au, E_{em} = 508 nm, (E_{ex} = 428 nm). ESI-MS (m/z): 769 [$M - H + 2Li$] $^+$.

PS-Trisamine Dansyl-Lariat Ether Butylamine (1dw). (recovery 93%, conversion 98%). IR(KBr): 3025, 2923, 1577, 1451, 1317, 1140, cm^{-1} . FI = 767 au, E_{em} = 500 nm, (E_{ex} = 389 nm). ESI-MS(m/z): 579 [$M - C_2H_4 - NH_2 - R$] $^+$.

PS-Trisamine Dansyl-Lariat Ether Amylamine (1ew). (recovery 93%, conversion 96%). IR (KBr): 3018, 2923, 1577, 1457, 1319, 1140 cm^{-1} . FI = 852 au, E_{em} = 522 nm, (E_{ex} = 431 nm). ESI-MS (m/z): 685 [$M - NH_2 + Li$] $^+$.

Acknowledgment. We gratefully acknowledge support for this project by Consejo Nacional de Ciencia y Tecnología, México (CONACyT, Grant No. 28488-E) and Consejo Nacional de Educación Tecnológica, México (COSNET, Grant No. 23.97-P). Tania González²³ thanks CONACyT for a graduate fellowship.

References and Notes

- Gokel, G. W.; De Wall, S. L.; Barbour, L. J. *J. Am. Chem. Soc.* **1999**, *121*, 8405–8406.
- Sandanayake, A. S.; Sutherland, I. O. *Sens. Actuators* **1993**, *11*, 331–340.
- Vélez, E.; Pina-Luis, G.; Suárez, J. L.; Rivero, I. A.; Díaz-García, M. E. *Sens. Actuators, B* **2003**, *90*, 256–263.
- Yoon, J.; Czarnik, A. W. *J. Am. Chem. Soc.* **1992**, *114*, 5874.
- De Silva, P. A.; Fox, D. B.; Huxley, J. M.; Moody, T. S. *Coord. Chem. Rev.* **2000**, *41*, 203.
- Granda, M.; Badía, R.; Pina-Luis, G.; Díaz-García, M. E. *Quim. Anal.* **2000**, *19*, 38.
- De Silva, A. P.; de Silva, S. A. *J. Chem. Soc. Chem. Commun.* **1986**, *23*, 1709.
- De Silva, A. P.; Gunaratne, H. Q. N.; Gunnlångsson, T.; McKoy, C. P.; Maxwell, R. S.; Rademacher, J. T.; Rice, T. E. *Pure Appl. Chem.* **1996**, *48*, 1443.
- Kubo, K.; Sakaguchi, S.; Sakurai, T. *Talanta* **1999**, *49*, 735–744.
- Kubo, K.; Ishige, R.; Sakurai, T. *Talanta* **1999**, *49*, 339–344.
- Kubo, K.; Sakurai, T.; Mori, A. *Talanta* **1999**, *50*, 73–77.
- Cooper, C. R.; James, T. D. *J. Chem. Soc. Perkin Trans.* **2000**, *1*, 963–969.
- Ayadim, M.; Jiwan, J. H. L.; De Silva, A. P.; Soumillion, J. Ph. *Tetrahedron Lett.* **1996**, *37*, 7039.
- He, H.; Mortellaro, M. A.; Leiner, M. J. P.; Young, S. T.; Fraatz, R. J.; Tusa, J. K. *Anal. Chem.* **2003**, *75*, 549–555.
- He, H.; Mortellaro, M. A.; Leiner, M. J. P.; Fraatz, R. J.; Tusa, J. K. *J. Am. Chem. Soc.* **2003**, *125*, 1468–1469.
- Harris, R. F.; Nation, A. J.; Copeland, G. T.; Miller, S. J. *J. Am. Chem. Soc.* *122*, 11270–11271.
- Rivero, I. A. *Av. Perspectiva* **1997**, *16*, 375–383.
- Rivero, I. A.; Somanathan, R.; Hellberg, L. H. *Synth. Commun.* **1993**, *23*, 711.
- Pina-Luis, G.; Badía, R.; Diaz-Garcia, M. E.; Rivero, I. A. *J. Comb. Chem.* **2004**, *6*, 391–397.
- Chavez, D.; Ochoa, A.; Madrigal, D.; Castillo, M.; Espinoza, K.; Gonzalez, T.; Velez, E.; Melendez, J. D.; Rivero, I. A. *J. Comb. Chem.* **2003**, *5*, 149–154.
- Shea, K. J.; Okahata, Y.; Dougherty, T. K. *Macromolecules* **1984**, *17*, 296–300.
- Li, Y.-H.; Chan, L.-M.; Tyer, L.; Moody, R. T.; Himel, C. M.; Hercules, D. M. *J. Am. Chem. Soc.* **1975**, *97*, 3118–3126.
- Fox, M. A.; Channon, M. *Photoinduced Electron-Transfer*; Elsevier: Amsterdam, 1998; parts A–D.
- Harriman, A.; Hissler, M.; Jost, P.; Wipff, G.; Ziessel, R. *J. Am. Chem. Soc.* **1999**, *121*, 14.
- Lehn, J. M. Design of Organic Complexing Agents. Strategies towards Properties. *Structure and Bonding*; Springer-Verlag: Berlin, 1973; Vol. 16, Chapter 1.
- Stewart, J. M.; Young, J. D.; Barany, G. *Solid-Phase Peptide Synthesis*; W. H. Freeman: San Francisco, 1969.

CC049897C